Blockade to pathological remodeling of infarcted heart tissue using a porcupine antagonist

Jesung Moon[a,1], Huanyu Zhou[b,c,1], Li-shu Zhang[c,d], Wei Tan[b,c], Ying Liu[e], Shanrong Zhang[f], Lorraine K. Morlock[g], Xiaoping Bao[h], Sean P. Palecek[h], Jian Q. Feng[e], Noelle S. Williams[g], James F. Amatruda[a,b,i], Eric N. Olson[b,c,2], Rhonda Bassel-Duby[b,c], and Lawrence Lum[c,d,2]

[a]Department of Pediatrics, University of Texas Southwestern Medical Center, Dallas, TX 75390; [b]Department of Molecular Biology, University of Texas Southwestern Medical Center, Dallas, TX 75390; [c]Hamon Center for Regenerative Science and Medicine, University of Texas Southwestern Medical Center, Dallas, TX 75390; [d]Department of Cell Biology, University of Texas Southwestern Medical Center, Dallas, TX 75390; [e]Department of Biomedical Sciences, Texas A&M University College of Dentistry, Dallas, TX 75246; [f]Advanced Imaging Research Center, University of Texas Southwestern Medical Center, Dallas, TX 75390; [g]Department of Biochemistry, University of Texas Southwestern Medical Center, Dallas, TX 75390; [h]Department of Chemical and Biological Engineering, University of Wisconsin Madison, Madison, WI 53706; and [i]Department of Internal Medicine, University of Texas Southwestern Medical Center, Dallas, TX 75390

Contributed by Eric N. Olson, December 28, 2016 (sent for review November 28, 2016; reviewed by Daniel J. Garry and Douglas L. Mann)

The secreted Wnt signaling molecules are essential to the coordination of cell-fate decision making in multicellular organisms. In adult animals, the secreted Wnt proteins are critical for tissue regeneration and frequently contribute to cancer. Small molecules that disable the Wnt acyltransferase Porcupine (Porcn) are candidate anticancer agents in clinical testing. Here we have systematically assessed the effects of the Porcn inhibitor (WNT-974) on the regeneration of several tissue types to identify potentially unwanted chemical effects that could limit the therapeutic utility of such agents. An unanticipated observation from these studies is proregenerative responses in heart muscle induced by systemic chemical suppression of Wnt signaling. Using in vitro cultures of several cell types found in the heart, we delineate the Wnt signaling apparatus supporting an antiregenerative transcriptional program that includes a subunit of the nonfibrillar collagen VI. Similar to observations seen in animals exposed to WNT-974, deletion of the collagen VI subunit, *COL6A1*, has been shown to decrease aberrant remodeling and fibrosis in infarcted heart tissue. We demonstrate that WNT-974 can improve the recovery of heart function after left anterior descending coronary artery ligation by mitigating adverse remodeling of infarcted tissue. Injured heart tissue exposed to WNT-974 exhibits decreased scarring and reduced Col6 production. Our findings support the development of Porcn inhibitors as antifibrotic agents that could be exploited to promote heart repair following injury.

Wnt | protein lipidation | heart regeneration | adult tissue homeostasis | extracellular matrix

The replacement of normal tissue with collagen-laden scars is a major impediment to wound recovery following injury. In heart tissue, a number of diverse disorders, including hypertrophic cardiomyopathy and heart failure, are associated with excessive deposition of fibrotic tissue (1). Whereas Wnt-mediated signaling is well established as a participant in maladaptive fibrotic responses in most tissues, including the heart (2), selective Wnt-signaling–targeted agents have been elusive, thus hampering efforts to pharmacologically exploit this understanding for intervention in heart disease.

Despite the multitude of cellular responses that they elicit, all 19 secreted Wnt family members are dependent upon the same biosynthetic enzymes, including Porcupine (Porcn), a multipass acyltransferase localized to the endoplasmic reticulum (ER) that supplies a single fatty acid adduct necessary for Wnt protein exit from the secretory pathway (3–6). Transport of Wnt protein to the cell surface from the ER requires interaction of the putative lipoprotein receptor Wntless, a seven-transmembrane protein that facilitates acylated Wnt protein secretion (7). Thus, Wnt proteins that fail to be acylated are unable to exit the ER and are unable to reach various Wnt receptors found on the cell surface.

From a small-molecule screen for Wnt pathway inhibitors, Porcn emerged as a highly druggable target (8). Despite the intense interest in Porcn inhibitors as anticancer agents, the importance of Wnt signaling in diverse cell types—including fibroblasts, which produce connective tissue—suggests that such agents could be useful in regenerative medicine (9). Here we have applied the clinical candidate Porcn inhibitor (WNT-974) to characterize the response of diverse tissues to transient chemical suppression of Wnt signaling. Although some tissues were predictably compromised by loss of Porcn activity, heart muscle tissue saw increases in the mitotic activity of cells responsible for regeneration. We delineate, using in vivo and in vitro approaches, the autonomous and noncell-autonomous Wnt signals that support an antiregenerative state in adult heart tissue. Using WNT-974, we demonstrate that infarcted heart tissue with suppressed Wnt signaling shows decreased scarring and improved heart function. We focus here on the profibrotic molecule collagen VI as an effector protein complex of proregenerative activities induced by Porcn inhibitors in heart cells.

Results

An in Vivo Screen to Identify Tissues Sensitive to Porcn Inhibitors. In an effort to anticipate dose-limiting toxicities associated with the use of Porcn inhibitors in clinical settings, we evaluated the sensitivity of various murine adult tissues to WNT-974 exposure at a dosage that previously has been associated with anticancer activity but little toxicity (10, 11) (Fig. 1*A*). Given the central role of Wnt signaling in gut epithelium renewal (12), we first confirmed

Significance

A significant factor influencing longevity and quality of life in heart attack survivors is the extent of adverse tissue remodeling in injured heart tissue, which impedes mechanical function and accelerates the progression of heart failure. Despite the general consensus that mitigating fibrotic responses would delay the onset of heart failure and improve heart function after a heart attack, there currently are no agents that directly target this pathological process available for heart disease management. Here we demonstrate that chemical inhibition of the Wnt acyltransferase Porcupine results in improvements in heart function following myocardial infarction in mice. Our findings advocate for the development of Porcupine inhibitors as proregenerative agents in the heart and other tissues.

Author contributions: J.M., H.Z., L.-s.Z., J.F.A., R.B.-D., and L.L. designed research; J.M., H.Z., L.-s.Z., W.T., Y.L., S.Z., L.K.M., X.B., and N.S.W. performed research; J.M., X.B., and S.P.P. contributed new reagents/analytic tools; J.M., H.Z., W.T., Y.L., S.Z., X.B., S.P.P., J.Q.F., J.F.A., E.N.O., R.B.-D., and L.L. analyzed data; and J.M., H.Z., R.B.-D., and L.L. wrote the paper.

Reviewers: D.J.G., University of Minnesota; and D.L.M., Washington University School of Medicine.

The authors declare no conflict of interest.

[1]J.M. and H.Z. contributed equally to this work.

[2]To whom correspondence may be addressed. Email: Eric.Olson@utsouthwestern.edu or lawrence.lum@utsouthwestern.edu.

This article contains supporting information online at www.pnas.org/lookup/suppl/doi:10.1073/pnas.1621346114/-/DCSupplemental.

the absence of weight change in animals treated using this drug-delivery protocol (Fig. 1*B*). However, consistent with the importance of Wnt signaling in the gut epithelium, we noted a loss in the number of proliferating cell nuclear antigen-positive ($PCNA^+$) cells in the jejunum crypt cells, which is indicative of decreased mitotic activity (Fig. 1*C* and Fig. S1). These results suggest that in the presence of cyclic exposure to Porcn inhibitors, gut epithelial stem and progenitor cells are nevertheless able to sustain tissue renewal.

We examined the effects of systemic WNT-974 exposure on two other tissues that are reliant upon Wnt signaling for regeneration: hair follicles and cartilage (13, 14). In both tissue types, suppression of Wnt signaling, following either depilation or the introduction of puncture wounds in the ear, resulted in delayed hair and cartilage regrowth (Fig. 1 *D* and *E*). Given the well-established role of Wnt/β-catenin signaling in promoting bone formation (15), we then determined the effects of Porcn inhibition on bone density as measured in the tibia midshaft (Fig. 1*F* and Fig. S2) and metaphasis (Fig. S3). A notable loss of bone mass was observed, suggesting bone health should be monitored in cases where Porcn inhibitors may be used long-term. Thus, a chemical agent targeting Porcn exhibits anticipated on-target effects in several tissues that likely stem from loss of Wnt signaling.

Unexpectedly, heart tissue exposed to WNT-974 displayed an increase in the mitotic activity of cardiomyocytes (CMs), suggesting that health of the myocardium may be improved from suppression of Wnt ligand expression (Fig. 1*G*). Taken together with conclusions drawn from other in vivo studies using Porcn inhibitors (11, 16, 17), our observations reveal potential dose-limiting on-target activities of Porcn inhibitors in adult mammals, but also reveal possible proregenerative cellular activity in heart tissue with decreased Wnt protein production (Fig. 1*H*).

WNT-974 Alters the Expression of Profibrotic Genes in the Heart. The recalcitrance of adult CMs to reentering the cell cycle poses a significant challenge to the development of agents that directly promote wound healing in heart tissue (18). We exploited the responsiveness of homeostatic heart tissue to WNT-974 exposure to identify Wnt-regulated cellular processes that may suppress CM cell cycle reentry. Tissues exposed to WNT-974 exhibit a significant change in expression of genes that contribute to remodeling of the extracellular matrix (ECM), including several that are associated with Wnt/β-catenin signaling (14, 19–21) (Fig. 2*A* and Dataset S1). For example, the secreted Wnt/β-catenin signaling antagonist Dkk3 suppresses maladaptive remodeling of infarcted tissue in mice and protects against cardiac dysfunction after injury (22). The decreased expression of the Col6 subunit (Col6a3) is also notable, given that Col6 has been shown to suppress heart regeneration in injured murine heart tissue (23). Animals null for *COL6A1* show a marked improvement in heart function and decreased scarring following left anterior descending

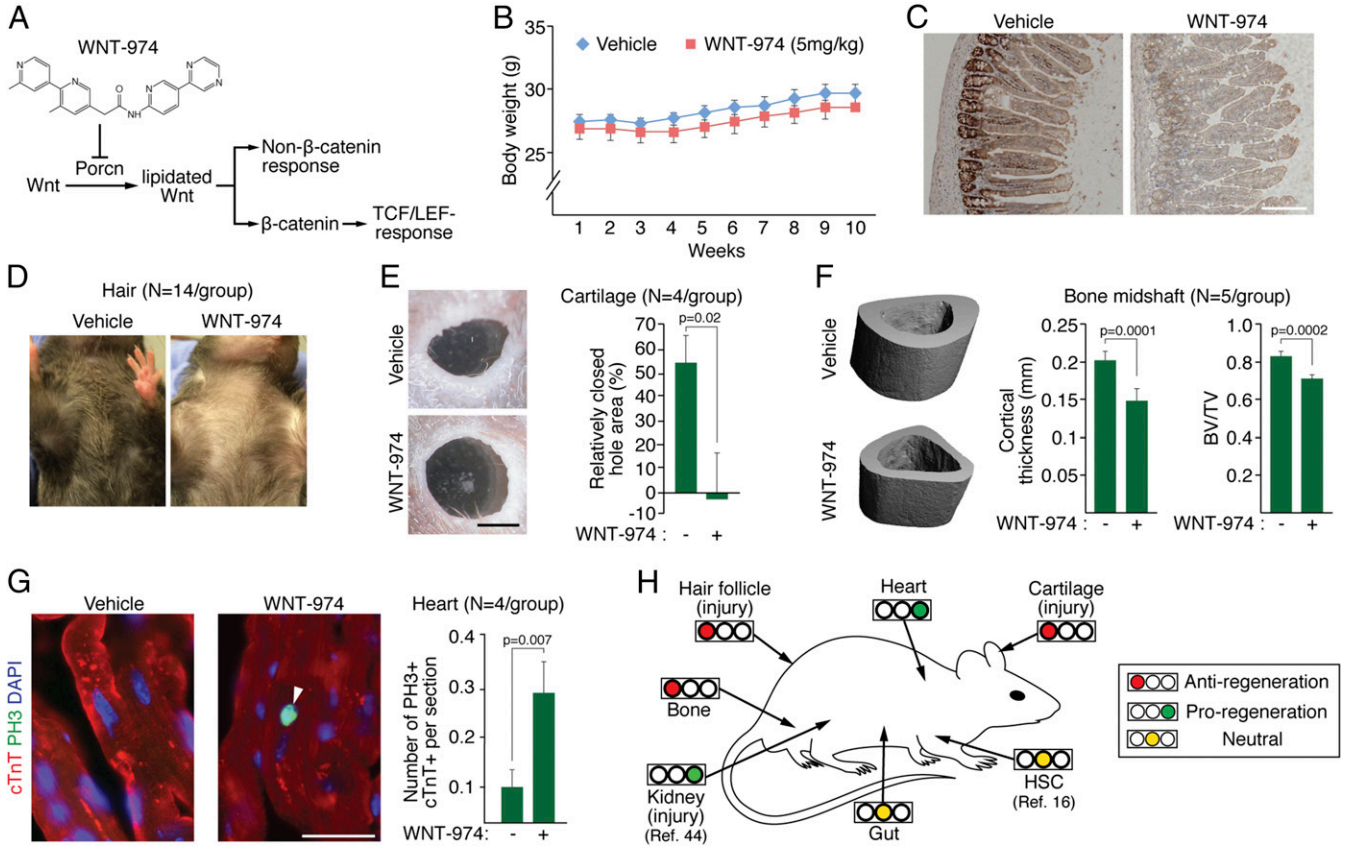

Fig. 1. Systematic identification of Porcn inhibition sensitivity in tissue regeneration. (*A*) The phase II clinical candidate WNT-974 inhibits both β-catenin–dependent and –independent cellular responses. The TCF/LEF family of transcriptional regulators is directly activated by β-catenin. (*B*) WNT-974 dosed at 5 mg/kg has little/no effect on animal weight compared with vehicle-treated animals. (*C*) PCNA staining of jejunum tissue derived from WNT-974 and vehicle-treated animals. (Scale bar, 200 μm.) (*D*) Animals treated with WNT-974 (10 wk) fail to regrow hair after waxing compared with vehicle-treated animals. (*E*) Animals treated with WNT-974 have delayed wound closure in the ear. Two-square millimeter ear hole punches were generated in vehicle and WNT-974–treated animals and the area of unrecovered tissue measured 20 d later. (Scale bar, 1 mm.) (*F*) Representative 3D images of tibia midshaft cortical bone generated using microcomputed tomography (μCT) in vehicle- or WNT-974–treated animals (10 wk). Bone volume fraction determination in the tibia midshaft using μCT. (*G*) Doubling CMs ($cTnT^+$, cardiac-specific isoform of troponin T; $PH3^+$, marker for mitosis) are increased in WNT-974–treated animals (3 wk). Twenty sections per animal were quantified. (Scale bar, 20 μm.) (*H*) A summary of adult tissue sensitivities to WNT-974 (or precursor molecule) presented in this study and by other research groups at a concentration of 3–5 mg/kg. All tissues were analyzed under homeostatic conditions, unless otherwise indicated.

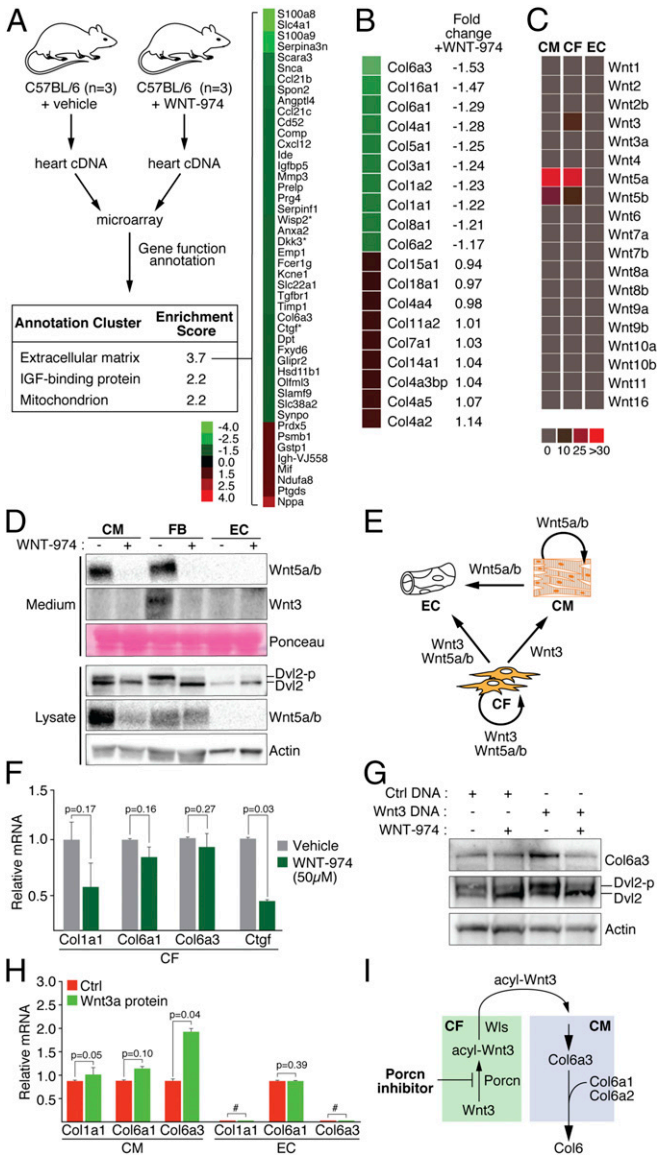

Fig. 2. WNT-974 induces changes in ECM regulatory gene expression in normal heart tissue. (*A*) ECM composition in heart tissue is likely altered in the presence of WNT-974. cDNA derived from 3× animals treated with vehicle or WNT-974 was subjected to microarray analysis. DAVID software (48) was used to identify cellular processes that were altered by exposure to WNT-974 (with genes ≥1.5 fold-change). Asterisks (*) denote known targets of Wnt/β-catenin signaling or signaling regulators. (*B*) Expression changes in collagen family members introduced by WNT-974 exposure in heart tissue. (*C*) qPCR profiling of Wnt molecules expressed in three major heart resident cell types cultured in vitro. CMs were generated from induced pluripotent stem cells; ECs and CFs are primary cells from human heart tissue. (*D*) CFs exhibit the most robust cell-autonomous Wnt signaling as measured using phosphorylation of the Dvl2 signaling molecule, a general marker of Frizzled receptor activation by Wnt proteins. WNT-974 decreased the abundance of secreted Wnt proteins in the culture medium and turnover of presumably unlipidated Wnt protein in the secretory pathway. (*E*) A map of potential Wnt-mediated cell-to-cell signaling interactions among the three most abundant heart cell types. (*F*) Inhibition of cell-autonomous Wnt signaling in CFs using a high concentration of WNT-974 does not alter Col6 expression as measured by Col6a1 and Col6a3 mRNA abundance. CTGF is a target gene of Wnt/β-catenin signaling. CFs are known to express Col1, an abundant ECM protein found in heart tissue (25). (*G*) Col6 expression in CMs as determined using Western blot analysis is controlled by lentivirus-mediated introduction of Wnt3 DNA. Loss of cell autonomous Wnt5a/b signaling induced by WNT-974 exposure does not impact Col6 expression (see *E*). Dvl2 phosphorylation serves as a marker of cell-autonomous Wnt signaling status. (*H*) Purified Wnt3a protein induces transcriptional activation of Col6 gene expression in CMs but not ECs. # denotes undetectable. (*I*) A model of antiregenerative Wnt signaling in heart tissue that is disabled by Porcn antagonists. Wntless (Wls) is a chaperone protein that facilitates the exiting of acylated Wnt proteins.

(LAD) ligation, as in the case of WNT-974–treated animals. Similar to other collagen proteins, a Col6 monomer comprises three subunits (Col6a1, -a2, -a3) that are assembled in stoichiometric fashion in the secretory pathway (24). Recessive mutations associated with Ullrich congenital muscular dystrophy found in a single subunit of Col6 are sufficient to eliminate the production of Col6 microfibrils, thus revealing the importance of coordinated subunit expression (24). Notably, among the collagen gene family members including those abundantly expressed in heart tissue, such as Col1 and Col3, the expression of Col6a3 was the most impacted by the presence of WNT-974 (Fig. 2*B*) (25).

Wnt Signaling in the Heart. CMs, cardiac fibroblasts (CFs), and endothelial cells (ECs) constitute the three major resident cell types found in the murine heart, with ECs and CFs comprising ∼80% of the non-CM resident cells (26). We characterized the Wnt expression profile in these cells using either cultured primary ECs and CFs, or CMs generated from induced pluripotent stem cells (27). CMs engineered using this protocol have been shown to faithfully model drug responses in heart tissues, exhibit electrophysiological characteristics of true CMs, and can be stably engrafted in living heart tissue (28–31). The expression of only three Wnt genes was detectable using a quantitative PCR (qPCR) strategy in these cells: Wnt5a/b in CFs and CMs, and Wnt3 in CFs (Fig. 2*C*). Western blot analysis of Wnt5a/b and Wnt3 protein in the medium of cultured cells confirmed that Wnt proteins were indeed produced and secreted in CFs and CMs, suggesting they are lipidated and functional (Fig. 2*D*). The levels of phosphorylated Dishevelled 2 (Dvl2) protein, an activity reporter of the Frizzled family of Wnt receptors (32), mirror those of the abundance of secreted Wnt protein produced by each cell type (Fig. 2*C*). We note that WNT-974 decreased the levels of Wnt protein in the culture medium without inducing an accumulation of presumably unlipidated Wnt protein in the secretory pathway. Along with an absence of enriched expression changes in genes associated with unfolded protein response (Table S1), we conclude that WNT-974 does not induce ER stress. Taken together, our in vitro studies reveal cell-autonomous and potential noncell-autonomous signaling events that would be disabled by WNT-974 exposure in intact heart tissue (Fig. 2*E*). These observations also suggest that among the three major resident cell types in the heart, CFs likely exhibit the most pronounced response to Porcn inhibitors in vivo.

As in other tissue types, fibroblasts found in the heart dictate the composition of the ECM (33). Given that CFs elaborate the entire repertoire of Wnt molecules expressed among the three major resident heart cell types (Fig. 2*C*), we determined if suppression of Wnt production by treatment with WNT-974 is sufficient to inhibit the expression of the Col6 subunits Col6a1 or Col6a3 (Fig. 2*F*). Despite the use of an excessively high concentration of WNT-974, we observed loss in the expression of the matricellular gene connective tissue growth factor (CTGF), a Wnt/β-catenin target gene (34), and a subunit of collagen 1 (Col1), but little change in the expression of Col6a1/a3.

To identify the non-CF cell type that exhibits WNT-974–sensitive Col6 expression, we first determined if suppression of cell-autonomous Wnt5a/b signaling in CMs using WNT-974 affected Col6 expression (Fig. 2*G*). Although we saw no change in Col6 expression when WNT-974 was added alone, introduction of Wnt3 expressing DNA into CMs induced Col6 in a WNT-974–dependent manner. Our detection of changes in Col6a1 and Col6a3 transcript abundance in CMs treated with recombinant Wnt3a reveals a transcriptional activation-dependent mechanism of Col6 expression controlled by Wnt signaling (Fig. 2*H*). On the

other hand, ECs failed to respond to Wnt3a protein, suggesting that CMs are the primary effector cells of WNT-974 action at least with respect to Col6 expression. When taken together, our observations suggest that Porcn inhibitors inhibit Wnt3 protein production from CFs, thus reducing the production of Col6 expression in CMs (Fig. 2*I*).

Chemical Inhibition of Porcn Improves Heart Function Recovery Following Myocardial Infarction. The effects of WNT-974 in decreasing the expression of profibrotic genes, such as Col6, suggests that targeting Porcn may be a useful approach for promoting wound healing in infarcted heart tissue. We determined the effects of WNT-974 on recovery in infarcted heart tissue provoked by permanent ligation of the LAD coronary artery. In two blinded studies, animals were equally segregated into cohorts for vehicle or WNT-974 treatment based on echocardiography (Fig. S4) or MRI (Fig. 3*A*, Fig. S5, and Table S2) following LAD ligation. Although area at risk was not measured, the extent of left ventricular dysfunction as measured by ejection fraction was similar in both groups before treatment, consistent with equivalent injury (Fig. 3*B*). Dosing of animals was initiated 1 wk following LAD occlusion, then continued for 10 wk. Animals treated with WNT-974 for 10 wk exhibited improved heart function compared with those treated with vehicle alone, as measured by ejection fraction (Fig. 3*B*). No change was observed in the heart rate of mice treated with WNT-974 compared with vehicle (Fig. 3*C*). We also noted that WNT-974 reduced injury-induced heart weight gain (Fig. 3*D*) and ventricular dilation (Fig. 3 *E* and *F*), which is consistent with improvements in heart function observed in the WNT-974–treated animals.

Porcn Inhibition Reduces Scarring in Heart Tissue. Histological examination of heart tissue revealed reduced scarring in animals with Wnt suppression (Fig. 4). We also observed a reduced number of CMs expressing Col6 in the infarcted area of mice treated with WNT-974 (Fig. S6). Notably, Col6 is not readily detected in uninjured heart tissue confirming that Col6 is induced following injury, as previously described (23). Taken together, these observations suggest Porcn inhibitors promote functional recovery of heart tissue primarily by mitigating scarring that may in part be attributable to loss in expression of the anti-regenerative molecule Col6.

Discussion

Wound repair in heart tissue is often described as a three-phase process composed of periods of inflammation, proliferation, and healing (35). The contribution of Wnt signaling in each of these phases is the subject of ongoing studies (36) and an understanding of these relationships has direct bearing on the optimal recovery response that can be ultimately achieved with Porcn inhibitors. Excessive deposition of collagen proteins in particular is problematic, given their slow turnover rate, which limits efforts to remove scar tissue once it is established (37). We show that the Porcn inhibitor WNT-974 prevents collagen production in CMs by blocking secretion of Wnt3, a profibrotic agonist, from CFs and its signaling to CMs.

Another study using a precursor compound of WNT-974 (GNF-6231) given at a comparable drug concentration recently reported similar proregenerative effects in heart tissue, including improvements in heart function following Porcn inhibition and reduced scarring (38). The immediate delivery of a Porcn inhibitor following LAD ligation in that study suggests that suppression of Wnt responses during the inflammatory phase does not contribute to the improvements in heart recovery seen in WNT-974–treated animals. At the same time, the success of our approach (a 1-wk delay in drug delivery following injury) reveals at a minimum a 1-wk window in which initiation of Porcn inhibitor delivery following myocardial infarction (MI) might be beneficial. Finally, we acknowledge that changes in the expression of Col6 may be only one proregenerative consequence of Porcn inhibition and that other molecular changes (38, 39) may also be factors that influence heart function outcome.

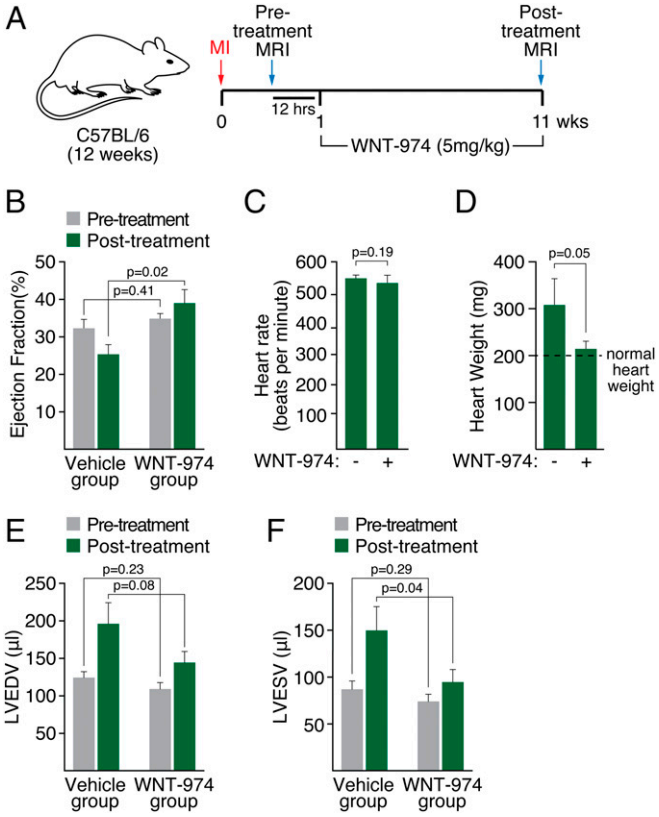

Fig. 3. Inhibition of Porcn improves heart function after LAD ligation. (*A*) Diagram showing strategy of procedure. One week following LAD ligation (MI), mice were subjected to MRI to determine pretreatment heart function. Mice were dosed with either WNT-974 (5 mg/kg; 1× by mouth each day) or vehicle for 10 wk. Heart function was then determined using MRI (posttreatment MRI). (*B*) Ejection fraction of pre- and posttreated mice. (*C*) Heart rate of vehicle or WNT-974–treated animals. (*D*) Heart weight of vehicle or WNT-974–treated animals. Normal heart weight for a 6-mo-old male C57BL/6 mouse is ∼200 mg (49). (*E*) Left ventricular end-diastolic volume (LVEDV) of vehicle or WNT-974–treated animals. (*F*) Left ventricular end- systolic volume (LVESV) of vehicle or WNT-974–treated animals.

Porcn inhibitors are likely to also target tissue-specific mechanisms supporting fibrosis or that suppress the activity of resident stem/progenitor cells. For example, epicardial cells responding to Wnt signals after injury have been shown to undergo epithelial-to-mesenchymal transition and adopt fibroblastic features in the subepicardium of injured neonatal heart tissue (40). Suppression of Porcn activity may blunt this phenomenon, in addition to influencing the activity of resident fibroblasts in the heart. A recent study using GNF-6231 also revealed potential increased doubling in the cardiac progenitor population following injury (38). Thus, activation of stem/progenitor cells by direct/indirect action of Porcn inhibitors may also contribute to improvements in regeneration in some tissues. Finally, although not addressed in this study, changes in the ECM composition because of Porcn inhibition may influence other heart repair processes, such as angiogenesis and inflammation (41).

Despite the importance of Wnt signaling in cancer and the intense interest in Porcn inhibitors as anticancer agents, the contribution of Wnt proteins in cell-fate decision making and in transcriptional regulation in fibroblasts suggests that such agents could be useful in other therapeutic arenas, including regenerative medicine (9). Our in vivo chemical screen using WNT-974 has identified a tissue that is not detrimentally affected by suppression of Wnt signaling and that may benefit from diminished fibrotic responses induced by Porcn inhibition. Indeed, other classes of small molecules with inhibitory activity for Wnt signaling have similarly shown

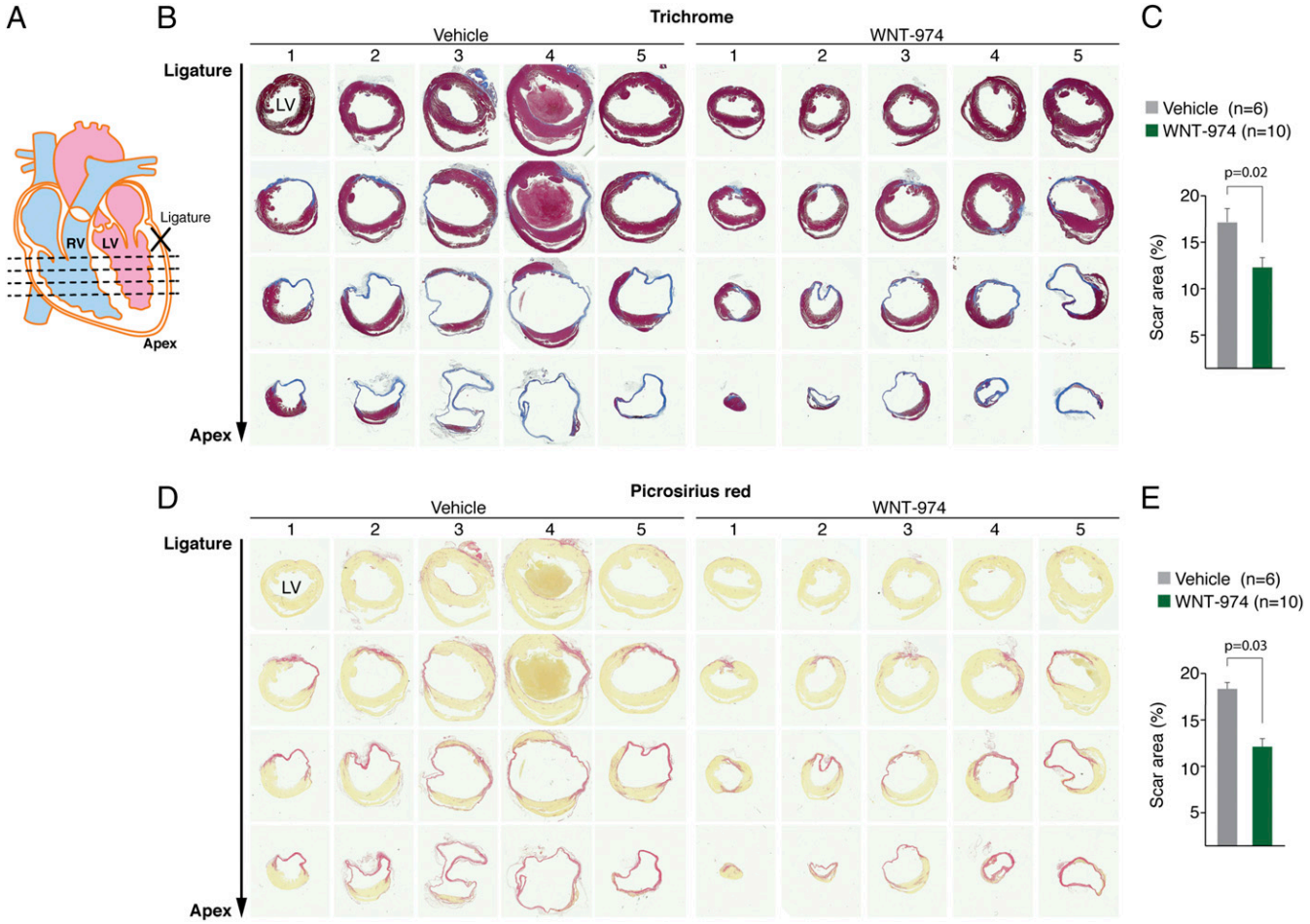

Fig. 4. Porcn inhibition reduces scarring in infarcted heart tissue. (*A*) Location of sections at four different levels relative to the LAD ligation position used for histological analysis of WNT-974– or vehicle-treated animals with LAD ligation. (*B*) Trichrome staining was used to visualize scar tissue in five different hearts from each animal treatment group. (*C*) Quantification of results in *B*. (*D*) Staining of heart sections with picrosirius red reveals decreased collagen deposition in WNT-974–treated animals. (*E*) Quantification of results in *D*.

beneficial responses in heart tissue; albeit, these molecules have not progressed further in clinical development for managing heart disease (42, 43). We also reason that other tissues, like the heart (Fig. 5), not yet fully investigated with Porcn inhibitors may also see similar benefits upon inhibition of Wnt ligand production. Indeed, these agents have been also shown to blunt kidney fibrosis induced by a murine model of obstructive nephropathy (44).

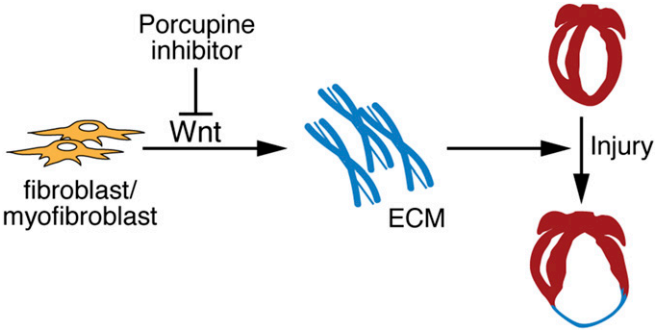

Fig. 5. A model for chemically assisted adult heart repair using Porcn inhibitor. Disruption of Wnt production in fibroblast/myofibroblasts by Porcn inhibitor reduces excess deposition of ECM proteins following heart injury, thus promoting heart repair.

Age-dependent increases in circulating Wnt molecules promote fibrotic responses at the cost of meaningful muscle restoration after injury (45). Life expectancy following heart attacks drops precipitously with increasing age after the age of 60 (46). Thus, an important next step is to demonstrate that proregenerative responses to Porcn inhibitors are preserved in aged animals. The use of such agents for tissue repair after injury will likely require transient chemical exposure, thus bypassing many of the on-target effects that may complicate the long-term delivery of these molecules in cancer management.

Materials and Methods

Wnt-974 Treatment. C57BL/6 mice [12-wk-old (LAD studies) or 3- to 12-mo-old (other studies)] were used. Wnt-974 (Active Biochem) was prepared in 0.5% (wt/vol) methylcellulose (Sigma)/0.5% (vol/vol) Tween-80 (Sigma) and administered by oral gavage at 5 mg/kg per mouse once per day for indicated time periods, as previously described (47). All animal experiments were performed in accordance to regulatory standards as accepted by the Institutional Animal Care and Use Committee at the University of Texas Southwestern Medical Center.

Microarray and qPCR. Methods for microarray and qPCR are described in *SI Materials and Methods*.

Bone Density Analysis. Micro-CT35 imaging system (Scanco Medical) was used to assess trabecular and cortical bone morphology. High-resolution scans (3.5-μm slice increments) of the long bone with 200 slices selected for analyses of the midshaft, and with 100 slices selected for analyses of the metaphysis area, were taken. The data were analyzed by using Scanco Medical software.

MI and Drug Treatment. Methods for MI and drug treatment are described in *SI Materials and Methods*.

Cardiac MRI. Methods for cardiac magnetic resonance imaging are described in *SI Materials and Methods*.

Histology and Immunostaining. Methods for histology and immunostaining are described in *SI Materials and Methods*.

Cell Culture, Recombinant Wnt Proteins, and Lentiviral Transduction. Methods for cell culture, recombinant Wnt proteins, and lentiviral transduction are described in *SI Materials and Methods*.

Western Blot Analysis. Methods for Western blot analysis are described in *SI Materials and Methods*.

Statistical Analysis. Values are displayed as mean ± SEM. Student's *t* test was performed for unpaired analysis. $P < 0.05$ was considered statistically significant.

Availability of Data and Materials. Our data and materials may be made available upon request to the corresponding author.

ACKNOWLEDGMENTS. We thank J. Cabrera for graphical assistance; J. Brown for administrative assistance; Shalini Muralidhar and Hesham Sadek for guidance with heart tissue immunohistochemistry; and Tom Shi for help with recombinant Wnt protein production. This work was supported by Robert A. Welch foundation Grants I-1665 (to L.L.) and 1-0025 (to E.N.O.); NIH Grants R01CA168761 (to L.L.), and HL-077439, DK-099653, AR-067294, HL-130253, and U01-HL-100401 (to E.N.O.); Cancer Prevention Institute of Texas Grants RP130212 (to L.L.) and RP110486 (to E.N.O.); and the Fondation Leducq Networks of Excellence (E.N.O.). H.Z. was supported by American Heart Association Pre-doctoral Fellowship 14PRE20030030.

1. Kong P, Christia P, Frangogiannis NG (2014) The pathogenesis of cardiac fibrosis. *Cell Mol Life Sci* 71(4):549–574.
2. Gourdie RG, Dimmeler S, Kohl P (2016) Novel therapeutic strategies targeting fibroblasts and fibrosis in heart disease. *Nat Rev Drug Discov* 15(9):620–638.
3. Bartscherer K, Boutros M (2008) Regulation of Wnt protein secretion and its role in gradient formation. *EMBO Rep* 9(10):977–982.
4. Kadowaki T, Wilder E, Klingensmith J, Zachary K, Perrimon N (1996) The segment polarity gene porcupine encodes a putative multitransmembrane protein involved in Wingless processing. *Genes Dev* 10(24):3116–3128.
5. Tanaka K, Okabayashi K, Asashima M, Perrimon N, Kadowaki T (2000) The evolutionarily conserved porcupine gene family is involved in the processing of the Wnt family. *Eur J Biochem* 267(13):4300–4311.
6. Willert K, et al. (2003) Wnt proteins are lipid-modified and can act as stem cell growth factors. *Nature* 423(6938):448–452.
7. Takada R, et al. (2006) Monounsaturated fatty acid modification of Wnt protein: Its role in Wnt secretion. *Dev Cell* 11(6):791–801.
8. Chen B, et al. (2009) Small molecule-mediated disruption of Wnt-dependent signaling in tissue regeneration and cancer. *Nat Chem Biol* 5(2):100–107.
9. Lum L, Chen C (2015) Chemical disruption of Wnt-dependent cell fate decision-making mechanisms in cancer and regenerative medicine. *Curr Med Chem* 22(35):4091–4103.
10. Juan J, Muraguchi T, Iezza G, Sears RC, McMahon M (2014) Diminished WNT -> β-catenin -> c-MYC signaling is a barrier for malignant progression of BRAFV600E-induced lung tumors. *Genes Dev* 28(6):561–575.
11. Liu J, et al. (2013) Targeting Wnt-driven cancer through the inhibition of Porcupine by LGK974. *Proc Natl Acad Sci USA* 110(50):20224–20229.
12. Clevers H (2013) The intestinal crypt, a prototype stem cell compartment. *Cell* 154(2):274–284.
13. Goldring MB, Marcu KB (2009) Cartilage homeostasis in health and rheumatic diseases. *Arthritis Res Ther* 11(3):224.
14. Lim X, Tan SH, Yu KL, Lim SB, Nusse R (2016) Axin2 marks quiescent hair follicle bulge stem cells that are maintained by autocrine Wnt/β-catenin signaling. *Proc Natl Acad Sci USA* 113(11):E1498–E1505.
15. Zhong Z, Ethen NJ, Williams BO (2014) WNT signaling in bone development and homeostasis. *Wiley Interdiscip Rev Dev Biol* 3(6):489–500.
16. Kabiri Z, et al. (2015) Wnts are dispensable for differentiation and self-renewal of adult murine hematopoietic stem cells. *Blood* 126(9):1086–1094.
17. Proffitt KD, Virshup DM (2012) Precise regulation of porcupine activity is required for physiological Wnt signaling. *J Biol Chem* 287(41):34167–34178.
18. Foglia MJ, Poss KD (2016) Building and re-building the heart by cardiomyocyte proliferation. *Development* 143(5):729–740.
19. Grünberg JR, Hammarstedt A, Hedjazifar S, Smith U (2014) The novel secreted adipokine WNT1-inducible signaling pathway protein 2 (WISP2) is a mesenchymal cell activator of canonical WNT. *J Biol Chem* 289(10):6899–6907.
20. Kessenbrock K, et al. (2013) A role for matrix metalloproteinases in regulating mammary stem cell function via the Wnt signaling pathway. *Cell Stem Cell* 13(3):300–313.
21. Si W, et al. (2006) CCN1/Cyr61 is regulated by the canonical Wnt signal and plays an important role in Wnt3A-induced osteoblast differentiation of mesenchymal stem cells. *Mol Cell Biol* 26(8):2955–2964.
22. Bao MW, et al. (2015) Dickkopf-3 protects against cardiac dysfunction and ventricular remodelling following myocardial infarction. *Basic Res Cardiol* 110(3):25.
23. Luther DJ, et al. (2012) Absence of type VI collagen paradoxically improves cardiac function, structure, and remodeling after myocardial infarction. *Circ Res* 110(6):851–856.
24. Bönnemann CG (2011) The collagen VI-related myopathies: Muscle meets its matrix. *Nat Rev Neurol* 7(7):379–390.
25. Eghbali M (1992) Cardiac fibroblasts: Function, regulation of gene expression, and phenotypic modulation. *Basic Res Cardiol* 87(Suppl 2):183–189.
26. Pinto AR, et al. (2016) Revisiting cardiac cellular composition. *Circ Res* 118(3):400–409.
27. Lian X, et al. (2013) Directed cardiomyocyte differentiation from human pluripotent stem cells by modulating Wnt/β-catenin signaling under fully defined conditions. *Nat Protoc* 8(1):162–175.
28. Bedut S, et al. (2016) High-throughput drug profiling with voltage- and calcium-sensitive fluorescent probes in human iPSC-derived cardiomyocytes. *Am J Physiol Heart Circ Physiol* 311(1):H44–H53.
29. Fonoudi H, et al. (2015) A universal and robust integrated platform for the scalable production of human cardiomyocytes from pluripotent stem cells. *Stem Cells Transl Med* 4(12):1482–1494.
30. Matsa E, et al. (2016) Transcriptome profiling of patient-specific human iPSC-cardiomyocytes predicts individual drug safety and efficacy responses in vitro. *Cell Stem Cell* 19(3):311–325.
31. Riegler J, et al. (2015) Human engineered heart muscles engraft and survive long term in a rodent myocardial infarction model. *Circ Res* 117(8):720–730.
32. Gao C, Chen YG (2010) Dishevelled: The hub of Wnt signaling. *Cell Signal* 22(5):717–727.
33. Baudino TA, Carver W, Giles W, Borg TK (2006) Cardiac fibroblasts: Friend or foe? *Am J Physiol Heart Circ Physiol* 291(3):H1015–H1026.
34. Luo Q, et al. (2004) Connective tissue growth factor (CTGF) is regulated by Wnt and bone morphogenetic proteins signaling in osteoblast differentiation of mesenchymal stem cells. *J Biol Chem* 279(53):55958–55968.
35. Liehn EA, Postea O, Curaj A, Marx N (2011) Repair after myocardial infarction, between fantasy and reality: The role of chemokines. *J Am Coll Cardiol* 58(23):2357–2362.
36. Deb A (2014) Cell-cell interaction in the heart via Wnt/β-catenin pathway after cardiac injury. *Cardiovasc Res* 102(2):214–223.
37. Rucklidge GJ, Milne G, McGaw BA, Milne E, Robins SP (1992) Turnover rates of different collagen types measured by isotope ratio mass spectrometry. *Biochim Biophys Acta* 1156(1):57–61.
38. Bastokoty D, et al. (May 30, 2016) Temporary, systemic inhibition of the WNT/β-catenin pathway promotes regenerative cardiac repair following myocardial infarct. *Cell Stem Cells Regen Med*, 10.16966/2472-6990.111.
39. Mohamed TM, et al. (November 10, 2016) Chemical enhancement of in vitro and in vivo direct cardiac reprogramming. *Circulation*, 10.1161/CIRCULATIONAHA.116.024692.
40. Mizutani M, Wu JC, Nusse R (2016) Fibrosis of the neonatal mouse heart after cryoinjury is accompanied by Wnt signaling activation and epicardial-to-mesenchymal transition. *J Am Heart Assoc* 5(3):e002457.
41. Shinde AV, Frangogiannis NG (2014) Fibroblasts in myocardial infarction: A role in inflammation and repair. *J Mol Cell Cardiol* 70:74–82.
42. Saraswati S, et al. (2010) Pyrvinium, a potent small molecule Wnt inhibitor, promotes wound repair and post-MI cardiac remodeling. *PLoS One* 5(11):e15521.
43. Sasaki T, Hwang H, Nguyen C, Kloner RA, Kahn M (2013) The small molecule Wnt signaling modulator ICG-001 improves contractile function in chronically infarcted rat myocardium. *PLoS One* 8(9):e75010.
44. Madan B, et al. (2016) Experimental inhibition of porcupine-mediated Wnt O-acylation attenuates kidney fibrosis. *Kidney Int* 89(5):1062–1074.
45. Brack AS, et al. (2007) Increased Wnt signaling during aging alters muscle stem cell fate and increases fibrosis. *Science* 317(5839):807–810.
46. Bucholz EM, et al. (2015) Life expectancy and years of potential life lost after acute myocardial infarction by sex and race: A cohort-based study of medicare beneficiaries. *J Am Coll Cardiol* 66(6):645–655.
47. Zhang LS, Lum L (2016) Delivery of the Porcupine inhibitor WNT974 in mice. *Methods Mol Biol* 1481:111–117.
48. Dennis G, Jr, et al. (2003) DAVID: Database for annotation, visualization, and integrated discovery. *Genome Biol* 4(5):3.
49. Doevendans PA, Daemen MJ, de Muinck ED, Smits JF (1998) Cardiovascular phenotyping in mice. *Cardiovasc Res* 39(1):34–49.
50. Liu TF, et al. (2012) Ablation of gp78 in liver improves hyperlipidemia and insulin resistance by inhibiting SREBP to decrease lipid biosynthesis. *Cell Metab* 16(2):213–225.
51. Yoshida Y, et al. (2003) Fbs2 is a new member of the E3 ubiquitin ligase family that recognizes sugar chains. *J Biol Chem* 278(44):43877–43884.
52. Ma Y, Hendershot LM (2004) Herp is dually regulated by both the endoplasmic reticulum stress-specific branch of the unfolded protein response and a branch that is shared with other cellular stress pathways. *J Biol Chem* 279(14):13792–13799.
53. Patra D, DeLassus E, Liang G, Sandell LJ (2014) Cartilage-specific ablation of site-1 protease in mice results in the endoplasmic reticulum entrapment of type IIb procollagen and down-regulation of cholesterol and lipid homeostasis. *PLoS One* 9(8):e105674.
54. Lavoie C, Meerloo T, Lin P, Farquhar MG (2002) Calnuc, an EF-hand Ca(2+)-binding protein, is stored and processed in the Golgi and secreted by the constitutive-like pathway in AtT20 cells. *Mol Endocrinol* 16(11):2462–2474.
55. Sun S, et al. (2014) Sel1L is indispensable for mammalian endoplasmic reticulum-associated degradation, endoplasmic reticulum homeostasis, and survival. *Proc Natl Acad Sci USA* 111(5):E582–E591.
56. Doroudgar S, et al. (2015) Hrd1 and ER-associated protein degradation, ERAD, are critical elements of the adaptive ER stress response in cardiac myocytes. *Circ Res* 117(6):536–546.

Supporting Information

Moon et al. 10.1073/pnas.1621346114

SI Materials and Methods

Microarray and qPCR. Total RNAs were extracted from hearts or cells with TRIzol reagent (Invitrogen) or RNeasy Kit (Qiagen) according to the manufacturer's instructions, respectively. cDNA was synthesized using RT2 HT first-strand kit (Qiagen) with 2 μg of RNA as a template. qPCR was performed using Lightcycler 480 (Roche). Relative fold-change was calculated using the ΔΔCt method after normalizing to Gapdh. Microarray analysis was performed by the University of Texas Southwestern Microarray Core facility using the MouseWG-6 V2.0 BeadChips (Illumina) using RNA extracted from heart samples and subsequently pooled before analysis.

MI and Drug Treatment. C57BL/6, 12-wk-old male mice, underwent permanent ligation of the LAD. Adult mice were anesthetized with isoflurane. Thoracotomy was performed at the third intercostal space, and self-retaining microretractors were placed to separate the third and fourth rib to visualize the LAD. The LAD was surgically ligated without tearing the pericardial sac. After LAD ligation, the retractors were removed and the chest was closed. Wnt-974 was administered by oral gavage at 5 mg/kg per mouse once per day for 10 wk.

Cardiac MRI. The cardiac function of mice was evaluated by cardiac MRI using a 7T small-animal MR scanner [Agilent (Varian)]. Under anesthesia by inhalation of 1.5–3% (vol/vol) isoflurane, the animals were placed prone on a mouse sled (Dazai Research Instruments) equipped with a pneumatic respiratory sensor and ECG electrodes for cardiac sensing, head first, with the heart centered with respect to the center of the RF coil. The chest area was shaved and a conducting gel was applied to optimize ECG contact between electrodes and mouse. All MRI acquisitions were gated using both cardiac and respiratory triggering. The bore temperature was kept at 33 ± 2 °C to assure adequate and constant heart rate. Axial images perpendicular to the long axis of the heart were chosen for Cine-imaging. Each scan consisted of five to nine contiguous slices from apex to left ventricle (LV) outflow with 1-mm thickness. Epicardial and endocardial borders were manually traced for calculation of left ventricular end systolic and end diastolic volumes (LVESV and LVEDV) using NIH ImageJ (v1.47j) software. Total LV volumes were calculated as the sum of all slice volumes. The LV ejection fraction (LVEF) was calculated by the equation, (LVEDV − LVESV)/LVEDV × 100%. Investigators performing MRI analysis were blinded to the assignment of mice in each group.

Histology and Immunostaining. Tissues were fixed in 4% (wt/vol) paraformaldehyde, embedded in paraffin, and cut 5-μm thick. For cryosection, hearts were fixed in 4% (wt/vol) paraformaldehyde for 1 h at room temperature and incubated in 30% (wt/vol) sucrose/PBS. Tissues were embedded in OCT medium, frozen at −80 °C. Cardiac fibrosis was evaluated by trichrome and picrosirius red staining 11-wk after MI injury. Heart sections were obtained starting at the level of 0.5 mm above the suture area and collected at three additional levels at a 1-mm interval. The stained sections were scanned by Artix Scan 4000tf. The images of the middle three levels were processed in Adobe Photoshop CS6 and analyzed in ImageJ to quantify blue-stained fibrotic areas. For immunostaining, sections were subjected to antigen retrieval and followed by staining against antibodies PCNA (Sigma; 1:100), cTnT (Millipore; 1:100), PH3 (Santa Cruz Biotechnology; 1:100), Col6a3 (Fitzgerald; 1:50). Conjugated antibodies (Alexa Fluor488 and 594, Invitrogen) were used as a secondary antibody. Images were taken with a Leica Microsystem 5500 microscope.

Cell Culture, Recombinant Wnt Proteins, and Lentiviral Transduction. Human CMs differentiated from human stem cells were provided by S.P.P. (University of Wisconsin at Madison, Madison, WI) and were grown in DMEM supplemented with 20% (vol/vol) FBS, in a 37 °C humidified incubator containing 5% CO_2. Human cardiac microvascular endothelial cells (Lonza) and human cardiac fibroblasts-adult ventricular (ScienCell) were cultured according to the manufacturers' instructions. After 16 h of serum starvation, cells were incubated for 4 h in the presence of 100 ng/mL recombinant mouse Wnt3a (Time Bioscience). Human WNT3-Lentiviral vector (pLV-mCherry:T2A:Puro-EF1A > hWNT3) was produced by VectorBuilder. Virus-containing media were collected after transfection into HEK-293T cells and used for transduction in the presence of >1 μg/mL Polybrene (Sigma).

Western Blot Analysis. Total cell lysates were prepared by lysing the cells with 2× sample loading buffer containing protease inhibitor mixture (Roche) and 2.5% (vol/vol) beta mercaptoethanol (Sigma). SDS/PAGE was conducted with antibodies against Wnt5a/b and Dvl2 (Cell Signaling Technology; 1:1,000), Wnt3 and Col6a3 (Santa Cruz Biotechnology; 1:1,000), β-actin (Sigma; 1:2,000). A LiCor Odyssey Fc instrument was used to detect chemiluminescent signal.

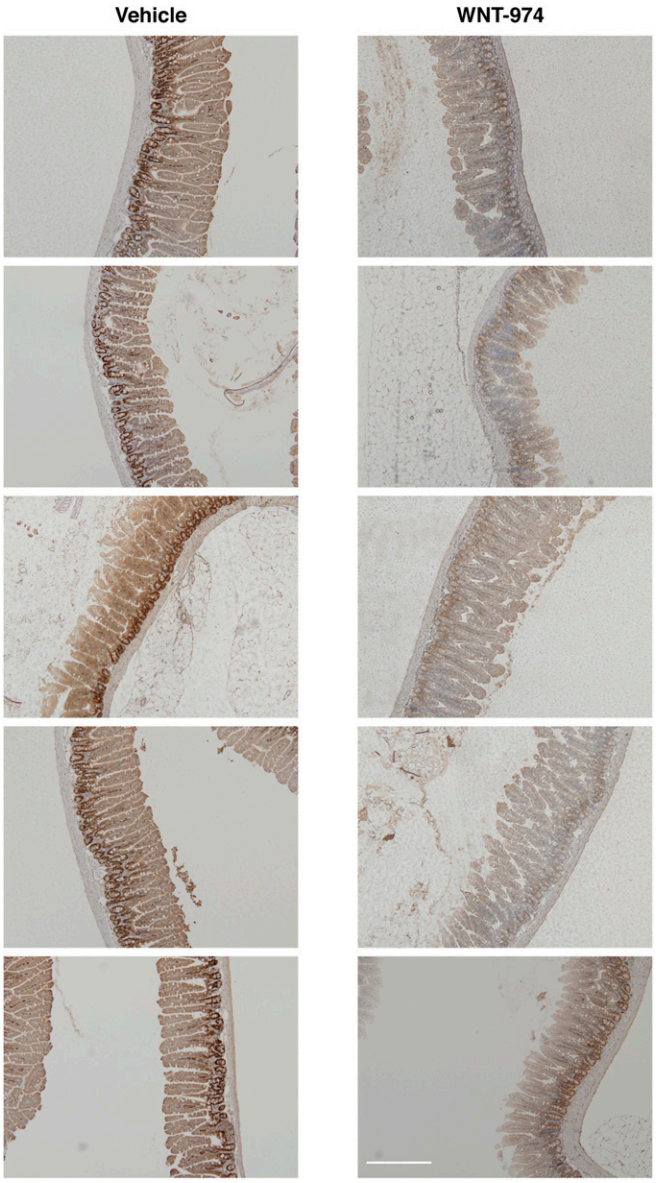

Fig. S1. Images of PCNA staining in gut tissue isolated from WNT-974 or vehicle-treated mice. (Scale bar, 200 μm.)

A	TV	BV	BV/TV	Mean/Density [mg HA/ccm] of BV (Material)	cortical thickness	cortical porosity
WNT974	0.3544	0.3431	0.9683	1006.1505	0.131	0.0317
WNT974	0.3725	0.3621	0.9722	1119.0068	0.148	0.0278
VEHICLE	0.4858	0.4771	0.982	1095.4897	0.207	0.018
VEHICLE	0.5385	0.5285	0.9813	1144.3771	0.204	0.0187
WNT974	0.3853	0.3753	0.974	1061.0449	0.147	0.026
VEHICLE	0.5079	0.499	0.9823	1141.5653	0.205	0.0177
WNT974	0.3685	0.3574	0.9701	1033.2463	0.155	0.0299
VEHICLE	0.509	0.4991	0.9806	1120.6045	0.198	0.0194
VEHICLE	0.4497	0.4415	0.9819	1080.4082	0.209	0.0181
WNT974	0.4167	0.4069	0.9764	1127.0588	0.154	0.0236

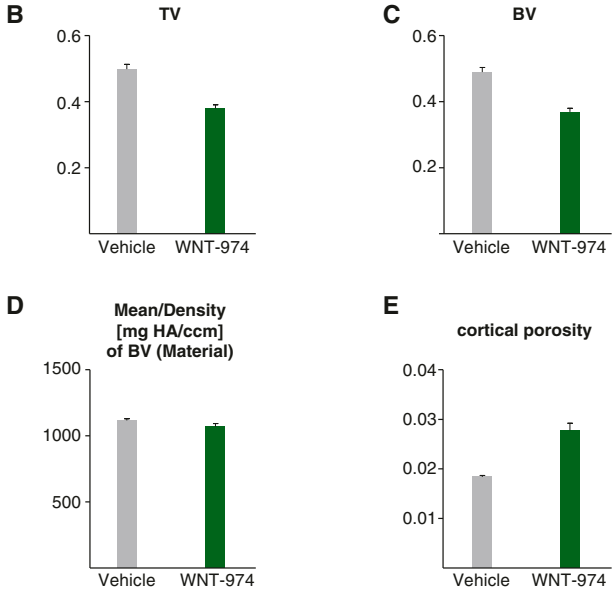

Fig. S2. Bone density measurements of tibia midshaft. (*A*) Data averaged from 200 sections of midshaft bone from mice treated with WNT-974 or vehicle generated using microcomputed tomography analysis. (*B*) Total volume (TV) of bone region measured. (*C*) Bone volume (BV) of region measured. (*D*) Density of BV. (*E*) Cortical porosity results.

A

Tibia metaphasis

	TV	BV	BV/TV	Mean/Density [mg HA/ccm] of BV (Material)
WNT974	1.1294	0.0325	0.0288	924.9912
WNT974	1.1369	0.0274	0.0241	921.093
VEHICLE	1.0802	0.0836	0.0774	922.1793
VEHICLE	1.1352	0.0945	0.0832	946.0798
WNT974	1.2217	0.0318	0.026	901.7936
VEHICLE	1.2302	0.1128	0.0917	920.6456
WNT974	1.0895	0.0718	0.0659	915.2776
VEHICLE	1.0953	0.0287	0.0262	937.8361
VEHICLE	1.3175	0.1187	0.0901	940.9674
WNT974	1.3011	0.0424	0.0326	938.4113

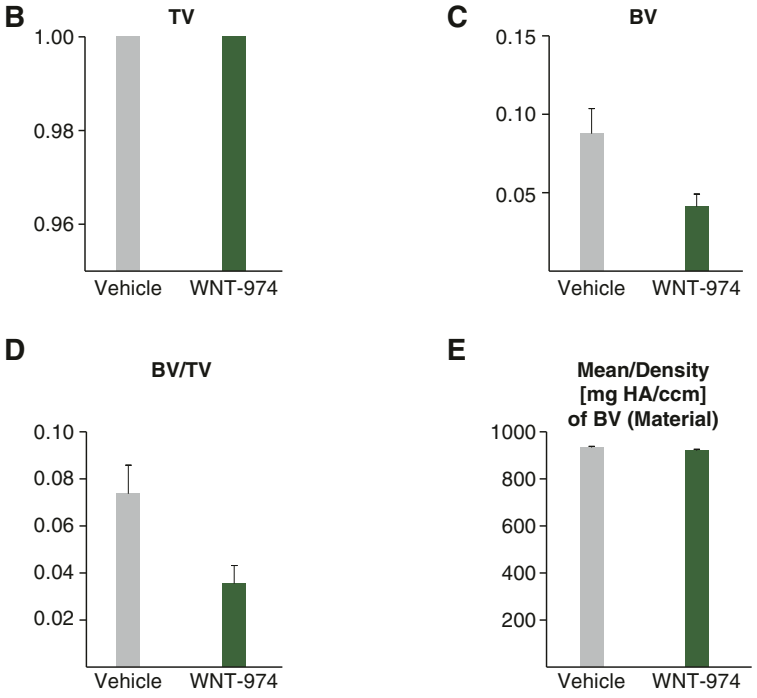

Fig. S3. Bone density measurements of tibia metaphysis. (*A*) Data averaged from 100 sections of metaphyses from mice treated with WNT-974 or vehicle generated using microcomputed tomography analysis. (*B*) Total volume (TV) of bone region measured. (*C*) Bone volume (BV) of region measured. (*D*) Ratio of BV/TV. (*E*) Density of BV.

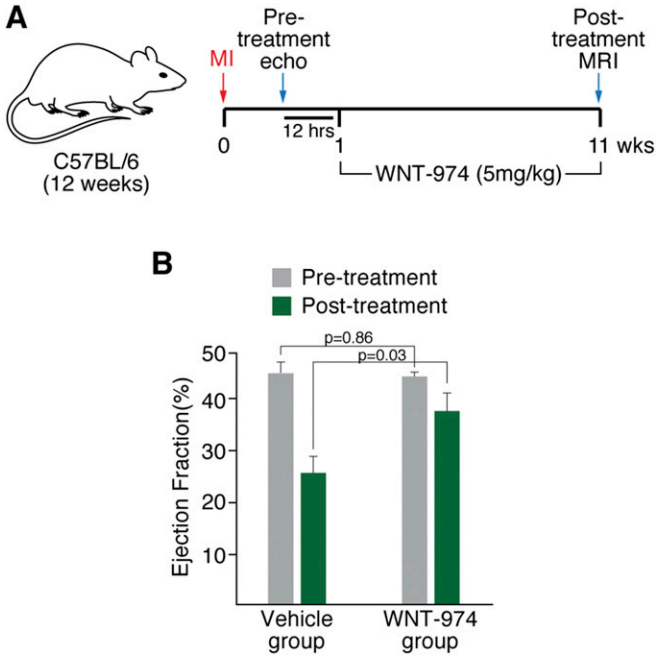

Fig. S4. Inhibition of Porcn improves heart function after LAD ligation. (*A*) Animals following LAD ligation with comparable heart function as determined using echocardiography ($n = 10$ per group) were dosed with either WNT-974 (5 mg/kg; 1× by mouth per day) or vehicle for 10 wk. Heart function of animals was then determined using MRI. (*B*) WNT-974–treated animals exhibit improved ejection fraction following LAD ligation.

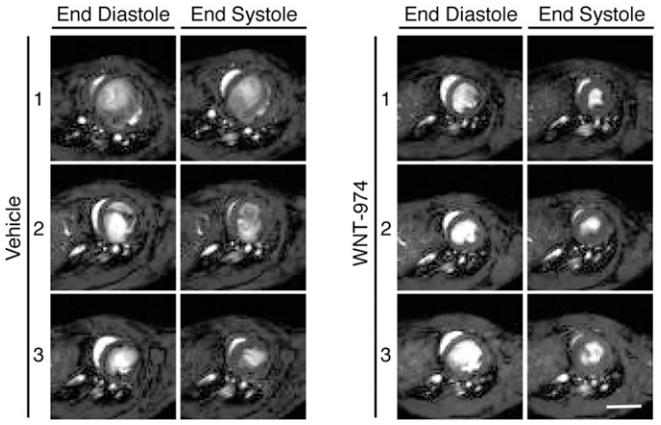

Fig. S5. MRI images of three mice treated with WNT-974 or vehicle. (Scale bar, 5 mm.)

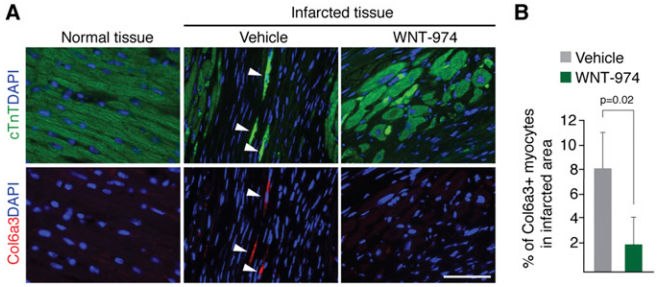

Fig. S6. Decreased expression of Col6a3 in cardiomyocytes exposed to WNT-974. (*A*) Heart tissue from LAD ligated animals were costained for Col6a3 and cTnT to identify the number of CMs expressing Col6a3 in the presence or absence of WNT-974. Normal tissue was derived from a remote area away from the site of infarction. (Scale bar, 50 μm.) (*B*) Quantification of Col6a3 positive myocytes in infarcted area of mice treated with WNT-974 or vehicle.

Table S1. Gene expression data for ER stress-related genes in heart tissue exposed to WNT-974 or vehicle derived from microarray analysis

Symbol	PROBE_ID	Vehicle	WNT-974	Fold-change	Acession	Source
Amfr	ILMN_2722902	1737.9	2027.6	1.17	NM_011787	Liu et al. (50)
Fbxo6b	ILMN_2660175	1881.4	1847.6	0.98	NM_015797.1	Yoshida et al. (51)
Herpud1	ILMN_2790246	3050.9	3209.5	1.05	NM_022331.1	Ma and Hendershot (52)
Mbtps1	ILMN_2748537	158.7	182.5	1.15	NM_019709.3	Patra et al. (53)
Nucb1	ILMN_2908735	359.9	343.7	0.95	NM_008749.1	Lavoie et al. (54)
Sel1l	ILMN_3137920	185.9	137.7	−1.35	NM_001039089.1	Sun et al. (55)
Syvn1	ILMN_2628258	1219.4	1294.1	1.06	NM_028769.4	Doroudgar et al. (56)

Table S2. MRI data for pre- and posttreated mice with WNT-974 or vehicle following LAD ligation

Group	Animal no.	EF (%)	HR (beat/min)	SV (μL)	CO(μL)	LVEDV(μL)	LVESV(μL)
Pretreatment (12 h before initial dosing)							
Vehicle	M2535	34.7	573.7	41.7	23.9	120.1	78.4
	M2541	19.2	563.2	31.4	17.7	163.9	132.4
	M2543	27.7	523.4	32.4	17.0	117.2	84.8
	M2553	28.7	523.9	36.5	19.1	127.1	90.5
	M2555	34.5	498.1	34.4	17.1	99.6	65.2
	M2557	43.5	519.7	44.1	22.9	101.6	57.4
	M2563	30.3	543.2	35.5	19.3	117.3	81.7
	M2564	21.9	551.8	35.8	19.8	163.4	127.5
	M2567	40.3	565.9	44.5	25.2	110.5	66.0
	Average	31.2	540.3	37.4	20.2	124.5	87.1
WNT974	M2530	49.3	458.0	36.4	16.7	73.8	37.4
	M2531	32.8	540.5	34.8	18.8	106.1	71.3
	M2534	47.1	550.4	42.4	23.3	89.9	47.6
	M2537	28.6	550.4	29.8	16.4	104.0	74.2
	M2542	38.4	588.1	28.6	16.8	74.6	46.0
	M2549	30.1	504.1	37.3	18.8	123.7	86.4
	M2550	29.7	545.3	35.3	19.2	118.8	83.6
	M2554	37.0	527.6	27.9	14.7	75.6	47.7
	M2556	37.2	526.3	27.5	14.5	74.0	46.5
	M2558	26.4	530.9	44.5	23.6	168.7	124.1
	M2560	31.2	559.2	40.2	22.5	128.9	88.7
	M2561	37.6	544.6	37.9	20.6	100.7	62.8
	M2562	32.5	521.6	36.1	18.8	111.1	75.0
	M2565	19.3	540.4	35.1	18.9	181.3	146.2
	M2568	32.3	534.9	35.3	18.9	109.0	73.7
	Average	34.0	534.8	35.3	18.8	109.3	74.1
Posttreatment (10-wk dosing)							
Vehicle	M2535	16.6	540.5	66.9	36.2	402.7	335.8
	M2541	21.8	576.7	49.8	28.7	228.5	178.7
	M2543	20.3	556.8	29.7	16.5	146.3	116.6
	M2553	30.2	582.4	54.4	31.7	179.9	125.5
	M2555	35.0	508.4	46.1	23.4	131.8	85.7
	M2557	20.9	582.4	36.1	21.0	173.1	137.0
	M2563	26.6	540.5	42.6	23.0	160.3	117.7
	M2564	23.6	479.8	48.9	23.5	207.5	158.6
	M2567	33.8	594.7	45.1	26.8	133.5	88.4
	Average	25.4	551.4	46.6	25.7	196.0	149.3
WNT974	M2530	61.4	483.8	48.7	23.6	79.4	30.7
	M2531	34.4	468.2	56.2	26.3	163.3	107.0
	M2534	52.5	559.9	57.5	32.2	109.5	52.0
	M2537	24.7	571.4	52.2	29.9	211.2	159.0
	M2542	56.2	479.6	47.9	23.0	85.2	37.3
	M2549	30.5	571.4	49.6	28.3	162.5	112.9
	M2550	20.6	576.7	28.0	16.2	136.1	108.1
	M2554	45.1	593.8	39.7	23.6	88.1	48.3
	M2556	26.6	550.4	25.1	13.8	94.3	69.2
	M2558	22.9	501.3	64.2	32.2	279.6	215.4
	M2560	42.6	333.1	77.8	25.9	182.6	104.8
	M2561	41.9	526.3	47.7	25.1	113.8	66.1
	M2562	41.0	523.5	50.0	26.2	122.1	72.1
	M2565	26.2	521.6	54.6	28.5	208.7	154.1
	M2568	36.1	576.7	45.3	26.1	125.4	80.1
	Average	37.5	522.5	49.6	25.4	144.1	94.5

Abbreviations: CO, cardiac output; EF, ejection fraction; HR, heart rate; LVEDV, left ventricular end-diastolic volume; LVESV, left ventricular end-systolic volume; SV, stroke volume.

Other Supporting Information Files

Dataset S1 (XLSX)